

10-2011

In vivo three-dimensional blood velocity profile shapes in the human common, internal, and external carotid arteries

Alexey Kamenskiy

University of Nebraska Medical Center, alexey.kamenskiy@unmc.edu

Yuris A. Dzenis

University of Nebraska-Lincoln, ydzenis@unl.edu

Jason N. MacTaggart

University of Nebraska-Medical Center, jmactaggart@unmc.edu


Anastasia Desyatova

University of Nebraska-Lincoln

Iraklis I. Pipinos

University of Nebraska Medical Center, ipipinos@unmc.edu

Follow this and additional works at: <http://digitalcommons.unl.edu/mechengfacpub>

 Part of the [Mechanics of Materials Commons](#), [Nanoscience and Nanotechnology Commons](#), [Other Engineering Science and Materials Commons](#), and the [Other Mechanical Engineering Commons](#)

Kamenskiy, Alexey; Dzenis, Yuris A.; MacTaggart, Jason N.; Desyatova, Anastasia; and Pipinos, Iraklis I., "In vivo three-dimensional blood velocity profile shapes in the human common, internal, and external carotid arteries" (2011). *Mechanical & Materials Engineering Faculty Publications*. 233.

<http://digitalcommons.unl.edu/mechengfacpub/233>

This Article is brought to you for free and open access by the Mechanical & Materials Engineering, Department of at DigitalCommons@University of Nebraska - Lincoln. It has been accepted for inclusion in Mechanical & Materials Engineering Faculty Publications by an authorized administrator of DigitalCommons@University of Nebraska - Lincoln.

In vivo three-dimensional blood velocity profile shapes in the human common, internal, and external carotid arteries

Alexey V. Kamenskiy, PhD,^a Yuris A. Dzenis, PhD,^a Jason N. MacTaggart, MD,^b Anastasia S. Desyatova, MS,^a and Iraklis I. Pipinos, MD,^b *Lincoln and Omaha, Neb*

Objective: True understanding of carotid bifurcation pathophysiology requires a detailed knowledge of the hemodynamic conditions within the arteries. Data on carotid artery hemodynamics are usually based on simplified, computer-based, or in vitro experimental models, most of which assume that the velocity profiles are axially symmetric away from the carotid bulb. Modeling accuracy and, more importantly, our understanding of the pathophysiology of carotid bifurcation disease could be considerably improved by more precise knowledge of the in vivo flow properties within the human carotid artery. The purpose of this work was to determine the three-dimensional pulsatile velocity profiles of human carotid arteries.

Methods: Flow velocities were measured over the cardiac cycle using duplex ultrasonography, before and after endarterectomy, in the surgically exposed common (CCA), internal (ICA), and external (ECA) carotid arteries (n = 16) proximal and distal to the stenosis/endarterectomy zone. These measurements were linked to a standardized grid across the flow lumina of the CCA, ICA, and ECA. The individual velocities were then used to build mean three-dimensional pulsatile velocity profiles for each of the carotid artery branches.

Results: Pulsatile velocity profiles in all arteries were asymmetric about the arterial centerline. Posterior velocities were higher than anterior velocities in all arteries. In the CCA and ECA, velocities were higher laterally, while in the ICA, velocities were higher medially. Pre- and postendarterectomy velocity profiles were significantly different. After endarterectomy, velocity values increased in the common and internal and decreased in the external carotid artery.

Conclusions: The in vivo hemodynamics of the human carotid artery are different from those used in most current computer-based and in vitro models. The new information on three-dimensional blood velocity profiles can be used to design models that more closely replicate the actual hemodynamic conditions within the carotid bifurcation. Such models can be used to further improve our understanding of the pathophysiologic processes leading to stroke and for the rational design of medical and interventional therapies. (J Vasc Surg 2011;54:1011-20.)

Atherosclerosis of the carotid artery bifurcation is a leading cause of stroke. Numerous studies link carotid bifurcation disease to the complex flow patterns present in the carotid bulb.¹⁻³ A sound understanding of carotid bifurcation pathophysiology and the design of ideal devices and techniques for treatment of carotid disease require thorough knowledge of the actual hemodynamic properties within the carotid artery. The hemodynamics of the carotid bifurcation are rather complex. The natural widening of the carotid bulb and the branching into the internal (ICA) and external carotid arteries (ECA) perturb the

normal laminar flow present in the more proximal common carotid artery (CCA).^{2,4} Flow alterations occur in both the longitudinal (parallel to the axis of the vessel) and transverse (perpendicular to the axis of the vessel) directions. In the longitudinal direction, flow in the bulb is partially reversed, a phenomenon termed boundary layer separation.^{2,4} In the transverse direction, flow undergoes considerable rotation, a condition known as secondary flow.^{2,4} Measurement of blood flow velocity vectors in the bulb is a challenging task because standard duplex examination is aimed to capture the longitudinal component of the velocity vector, providing no information on the transverse component or secondary flow.

Mathematical modeling can be utilized to overcome the complexities of direct hemodynamic measurements in the carotid bulb. Proximal and distal to the carotid bulb, flow is unidirectional with almost no boundary layer separation or secondary flow.⁴ Duplex ultrasound can accurately and precisely quantify the flow characteristics in these arterial segments and these measurements can be used as inflow (CCA measurements) and outflow (ICA and ECA measurements) boundary conditions for mathematical modeling of flow within the bulb. In addition to the center-luminal velocity, the shape of the velocity profile, its pulsatile characteristics, and geometry of the artery are also required knowledge for accurate modeling. These mathe-

From the Department of Engineering Mechanics, University of Nebraska-Lincoln,^a and the Department of Surgery, University of Nebraska-Medical Center.^b

This work was supported in part by NIH grants K08HL079967 and R01AG034995 and by the grants from Nebraska Research Initiative Nanofiber Core Facility, National Science Foundation, and UNL/UNMC Engineering for Medicine initiative.

Competition of interest: none.

Reprint requests: Iraklis I. Pipinos, MD, Department of Surgery, University of Nebraska Medical Center, 983280 Nebraska Medical Center, Omaha, NE 68198-3280 (e-mail: ipipinos@unmc.edu).

The editors and reviewers of this article have no relevant financial relationships to disclose per the JVS policy that requires reviewers to decline review of any manuscript for which they may have a competition of interest.

0741-5214/\$36.00

Copyright © 2011 by the Society for Vascular Surgery.

doi:10.1016/j.jvs.2011.03.254

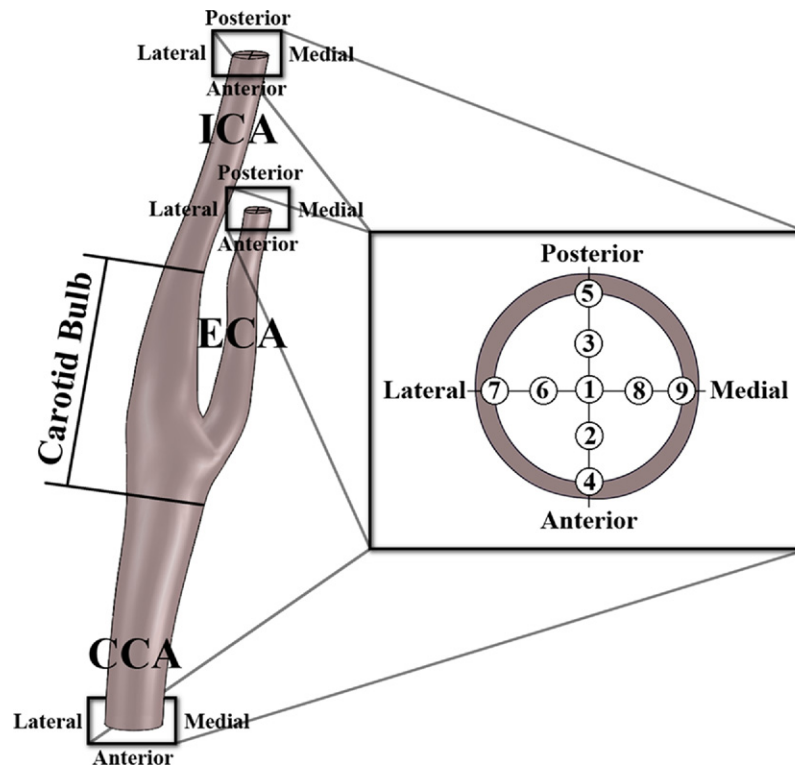


Fig 1. Schematic of a typical carotid bifurcation and locations of the points 1-9 where the velocity waveforms were measured. CCA, Common carotid artery; ECA, external carotid artery; ICA, internal carotid artery.

mathematical models can then be used to calculate and visualize the complex flow conditions within the carotid bulb.⁵

Most mathematical models that have been used to this point have significant limitations. In these models, velocity profiles are usually presumed symmetric about the arterial axis if measurements are made 4 to 5 vessel diameters from the flow divider.³ Even though it has recently been demonstrated that axisymmetric or fully developed flow appears to be the exception rather than the rule even in presumably straight CCA,⁶⁻⁸ typically velocities are still measured at one location in the center of the arterial lumen where flow is assumed to be the fastest. The remainder of the velocity profile is then calculated using axisymmetric parabolic or plug-shaped Womersley-type functions.⁴ This method is based on results obtained from idealized mathematical models and experiments using uniform, round, and rigid artificial vessels. However, while idealized geometry may be valuable for understanding certain flow phenomena, the in vivo carotid artery is rarely round, straight, or uniform in diameter.^{9,10} In addition, the geometry of the carotid artery varies from one patient to another.^{9,10} All of these factors may have pronounced effects on the shape of the velocity profiles^{2-4,11} and must be considered when developing mathematical flow models. The main reason why this assumption is widely used in modeling is lack of data in the literature that would report the details of the skewed shape of the CCA, ECA, and ICA velocity profiles.

We are presenting a systematic and detailed in vivo evaluation of velocity profiles in the human proximal CCA, distal ICA, and distal ECA from a series of patients undergoing carotid endarterectomy. All measurements were performed in vivo, in the surgically exposed carotid arteries before and after endarterectomy. To avoid limitations introduced by center-luminal velocity measurement alone, we measured velocities in nine different locations across the flow lumina of the CCA, ICA, and ECA (Fig 1). For each individual patient, three-dimensional, pulsatile velocity profiles were constructed and used to calculate mean velocity profiles for the preoperative and postoperative CCA, ICA, and ECA. In combination with geometrical data, these profiles can be used as flow boundary conditions for mathematical models studying the hemodynamics of the carotid artery.

METHODS

In vivo blood velocity measurements. The research protocol was approved by the institutional review board of the Veterans Affairs Nebraska-Western Iowa Medical Center and informed consent was obtained from all patients. Duplex ultrasound (Pro Focus 2202, Probe 8809; B-K Medical, Herlev, Denmark) evaluation of carotid artery blood flow was performed in 16 male patients (mean age, 67.9 ± 7.8 years) with severe (>80% diameter reduction) carotid bifurcation occlusive disease. None of the patients

had previous open or endovascular interventions performed on their carotids. Because of the improved resolution and optimal access to distal segments of the ICA and ECA, we chose to perform our measurements intraoperatively on the carotid bifurcation after it was exposed for the purposes of carotid endarterectomy. After exposure of the carotid bifurcation and control of the CCA, ICA, and ECA, preendarterectomy velocity measurements were obtained. After completion of the endarterectomy, closure of the arteriotomy, and re-establishment of flow, the postendarterectomy measurements were obtained. All patients were supine with arteries immersed in saline such that the ultrasound probe was not in physical contact with the artery during insonation. The systemic blood pressure was always within the normal range during ultrasound measurements. Mean preendarterectomy peak systolic pressure (PSP) was 126 ± 20 mm Hg, and end diastolic pressure (EDP) was 64 ± 9 mm Hg. Mean postendarterectomy PSP was 114 ± 16 mm Hg, and EDP was 58 ± 6 mm Hg. The arteries were fully dissected from surrounding tissues in their anterior, medial, and lateral aspects, and therefore the effect of surrounding tissues in the intraluminal flow velocities of the carotid arteries was not evaluated and was assumed to be minimal. Natural orientation of the carotid artery was preserved during insonation. We used the duplex to ascertain absence of residual stenosis or intimal flaps in CCA, ICA, and ECA prior to performing the postendarterectomy measurements. All operations and measurements were performed by the same vascular surgeon, and all patients received carotid endarterectomy using longitudinal arteriotomy and primary closure. Patients had a mean preoperative stenosis of 90% (range, 80%-95% based on measurements obtained from preoperative computerized tomographic angiography). Preoperative duplex ultrasound evaluation showed mean peak systolic velocity (PSV) of 371 ± 115 cm/s and end diastolic velocity (EDV) of 152 ± 35 cm/s. Mean ICA/CCA ratio was 5.2 ± 2.3 .

For each patient, velocity measurements were performed in three locations. The first location was 40 mm proximal to the flow divider in the CCA, the second in the ICA 50 mm distal to the flow divider, and the third in the ECA 30 mm distal to the flow divider. For the postendarterectomy ICA measurements, the location of the velocity measurements was at least 20 mm distal to end of the arteriotomy closure. These locations were chosen based on data describing the distance from the flow divider where flow reorganizes to become laminar. Chen¹¹ and Perktold³ report lengths of at least 4 to 5 arterial diameters. As the typical diameter of the common carotid artery is 5 to 8 mm and the usual diameters of the internal and external carotid arteries are 4 to 6 mm,^{12,13} based on these recommendations, velocity measurements should be performed at least 20 to 40 mm proximal to the carotid bulb in the CCA and 16 to 30 mm distal to the carotid bulb in the ICA and ECA.

At each of the three locations, velocity waveforms were measured at nine equally spaced points across the anterior-posterior and lateral-medial directions (Fig 1). Measurements in the anterior-posterior orientation were performed

with the probe positioned on top of the artery at the center of the anterior wall. The cursor on the duplex device screen was then moved within the lumen from the center to the anterior wall and then down to the posterior wall. Measurements in the lateral-medial orientation were taken by shifting the probe along the anterior wall of the artery laterally then medially, always keeping the cursor equidistance from the anterior and posterior walls of the artery.^{14,15}

Building three-dimensional velocity profiles. Blood velocity waveforms were digitized and entered into a specially developed Matlab code that interpolated axial velocity data across the cross-section of the vessel, providing information for precisely describing the full velocity profile. Interpolation was performed with third degree polynomials, ensuring a smooth distribution of velocity along the radial and circumferential directions of the arterial lumen. Thus, for each patient and each carotid branch, pre- and postendarterectomy three-dimensional pulsatile profiles were constructed. Since the length of the cardiac cycle was different for all patients, it was normalized to a 1 s cycle so that the mean velocity profile could be calculated. Similarly, because of differences in the diameters of the arteries, all measurements were scaled to a diameter of 1 cm.

RESULTS

In vivo blood flow profiles in the carotid artery

Pulsatile velocity profiles in the CCA, ICA, and ECA before and after endarterectomy were constructed from the in vivo duplex ultrasonographic data. Mean velocity profiles calculated from the data obtained from all 16 patients at specific cardiac cycle time points are presented in Figs 2-4. Scheme of the cardiac cycle and time points at which velocity data are presented is provided in each figure. Peak systole (PS) is the time of maximum flow, early diastole (ED) is the time of minimum flow, and late diastole (LD) is the end of the cardiac cycle.

Common carotid artery

Mean velocity profiles in the pre- and postendarterectomy common carotid artery are presented in Fig 2.

Anterior-posterior side

Systole. Peak systolic velocity increases by 15 cm/s after endarterectomy and its profile shape becomes more peaked. Both pre- and postendarterectomy profiles demonstrate higher systolic velocities posteriorly. Postendarterectomy peak systolic values close to the posterior wall are 19 cm/s higher than the velocities close to the anterior wall. This difference reaches statistical significance in the CCA, at peak systole ($P = .036$). Maximum systolic values are detected in the center lumen.

Diastole. Diastolic velocity values at late diastole are higher after endarterectomy, while the opposite is observed at early diastole. Early diastolic profiles are skewed toward the anterior wall. Posterior wall velocities however are still higher than anterior wall velocities. This result is statistically significant ($P = .023$) before endarterectomy at late dias-

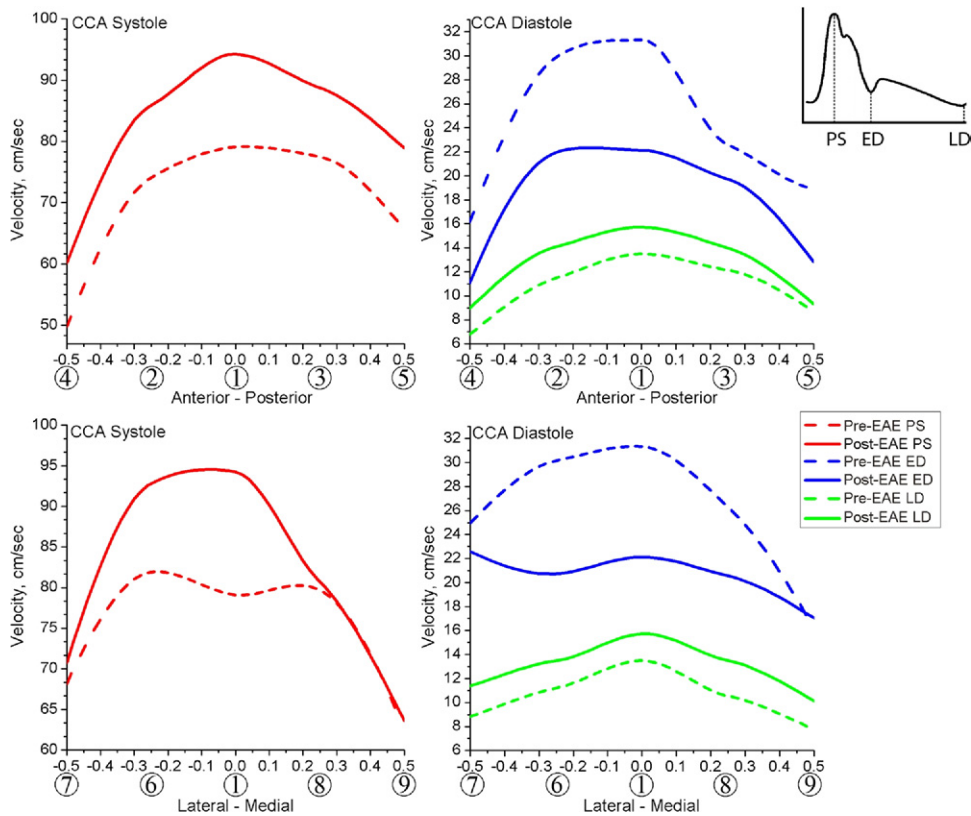


Fig 2. Mean velocity profiles in the common carotid artery (CCA) before and after endarterectomy (EAE). Data are presented at peak systole (PS), early diastole (ED), and late diastole (LD). Velocity profiles are given for two directions: anterior-posterior and lateral-medial. Numbers in circles along the horizontal axis represent points on Fig 1 where velocity waveforms were measured. Horizontal axis represents the diameter of the artery normalized to 1 cm.

tole. After endarterectomy profiles become more symmetric. Maximum velocity at early diastole is detected at the mid-distance between the center of the lumen and the anterior wall in both pre- and postendarterectomy conditions. Maximum values at late diastole are seen in the center lumen of the artery.

Lateral-medial side

Systole. Peak systolic velocity increases by 14 cm/s after endarterectomy, and the profile shape becomes more peaked. Both pre- and postendarterectomy profiles demonstrate higher systolic velocities laterally. The peak systole profile is skewed toward the lateral wall, and its shape changes from M-shaped before endarterectomy to parabolic-like after. Maximum velocities are detected mid-distance between the center of the lumen and the lateral wall.

Diastole. Velocity values for late diastole increase after endarterectomy but retain their profile. Velocity values for early diastole decrease after endarterectomy, and their profile becomes more flat with an increase of velocity at the lateral wall. During diastole, the early diastole velocity profiles are skewed toward the lateral wall while the late diastole profile remains fairly symmetric. Maximum velocity at early diastole is observed in the center lumen before

endarterectomy and moves toward the lateral wall after. Maximum velocity at late diastole is observed in the center lumen both before and after endarterectomy.

External carotid artery

Mean velocity profiles in the pre- and postendarterectomy external carotid artery are presented in Fig 3.

Anterior-posterior side

Systole. Peak systolic velocity decreased by 30 cm/s after endarterectomy. Both pre- and postendarterectomy profiles demonstrate higher systolic velocities posteriorly, but the difference between anterior and posterior values for the postendarterectomy carotid is more pronounced and equals 28 cm/s ($P = .041$). Maximum systolic values are detected in the center lumen.

Diastole. Diastolic velocity values at both early diastole and late diastole are lower after endarterectomy. Before endarterectomy at early diastole, the velocity profile has a peaked shape with higher velocities close to the anterior wall and maximum values in the center lumen. After endarterectomy, the velocity profile changes to the M-shaped with higher velocities posteriorly and maximum values

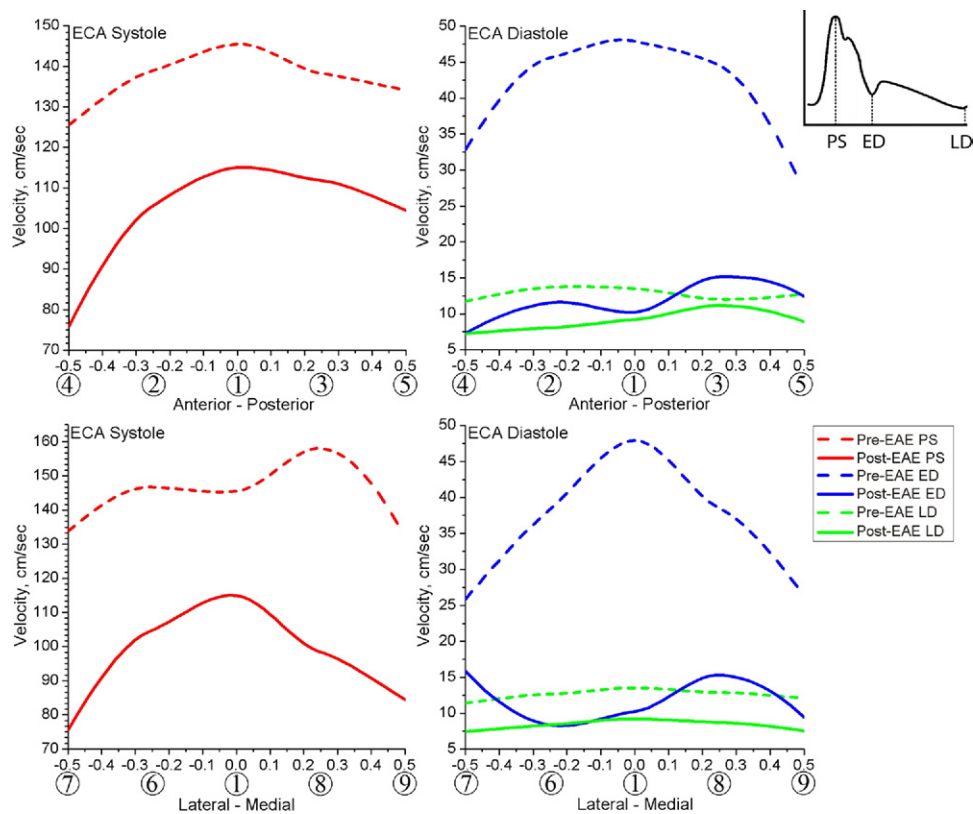


Fig 3. Mean velocity profiles in the external carotid artery (ECA) before and after endarterectomy (EAE). Data are presented at peak systole (PS), early diastole (ED), and late diastole (LD). Velocity profiles are given for two directions: anterior-posterior and lateral-medial. Numbers in circles along the horizontal axis represent points on Fig 1 where velocity waveforms were measured. Horizontal axis represents the diameter of the artery normalized to 1 cm.

observed between the center of the lumen and the posterior wall. Preendarterectomy profile at late diastole is almost flat with slightly higher values anteriorly. After endarterectomy, the profile reverses to the posterior side.

Lateral-medial side

Systole. Peak systolic velocity decreases by 30 cm/s after endarterectomy. The velocity profile changes from M-shaped to peaked, with maximum values moving from mid-distance between the center of the lumen and the medial wall preendarterectomy to the center of the lumen postendarterectomy. After endarterectomy, the velocity close to the medial wall is 9 cm/s higher than the velocity close to the lateral wall; however, the profile is skewed to the lateral side.

Diastole. Diastolic velocity values at both early diastole and late diastole are lower after endarterectomy than before. Before endarterectomy at early diastole, the velocity profile has a peaked shape with higher velocities close to the medial wall and maximum values in the center lumen. After endarterectomy, the velocity profile changes to a wave-shape with the highest velocities observed close to the lateral wall and mid-distance between the medial wall and the center lumen. Velocity values for late diastole decrease after endarterectomy but retain their profile.

Internal carotid artery

Mean velocity profiles in the preendarterectomy and postendarterectomy internal carotid artery are presented in Fig 4.

Anterior-posterior side

Systole. Peak systolic velocity increases by 12 cm/s after endarterectomy and its profile becomes more symmetric and spread-out. Both pre- and postendarterectomy profiles demonstrate higher systolic velocities posteriorly. Maximum systolic values are observed in the center lumen.

Diastole. Diastolic velocities are higher posteriorly. This is statistically significant for postendarterectomy ICA at late diastole ($P = .043$). At early diastole, the pre- and postendarterectomy velocities are relatively unchanged, with maximum values observed in the center lumen. However, the shape of the velocity profile after endarterectomy changes from peaked to a more symmetric and spread-out appearance. At late diastole, the profile also changes its shape from peaked to more blunt, with maximum velocity values observed at mid-distance between the posterior wall and the center lumen.

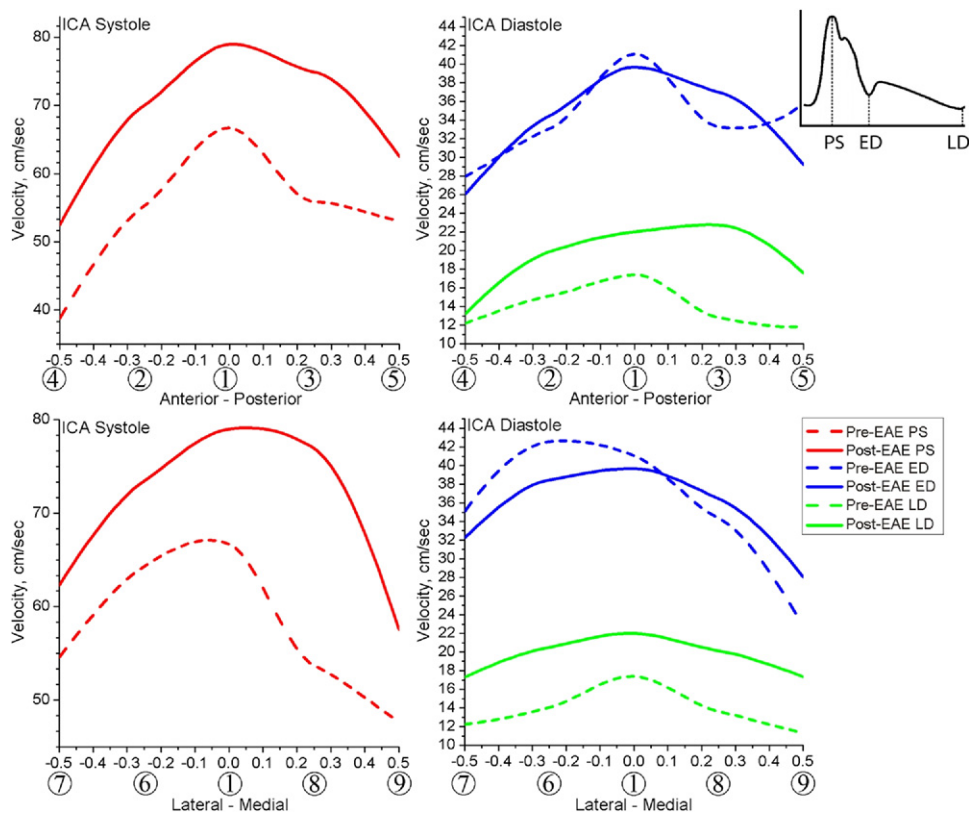


Fig 4. Mean velocity profiles in the internal carotid artery (ICA) before and after endarterectomy (EAE). Data are presented at peak systole (PS), early diastole (ED), and late diastole (LD). Velocity profiles are given for two directions: anterior-posterior and lateral-medial. Numbers in circles along the horizontal axis represent points on Fig 1 where velocity waveforms were measured. Horizontal axis represents the diameter of the artery normalized to 1 cm.

Lateral-medial side

Systole. Peak systolic velocity increases after endarterectomy. Preendarterectomy the velocity profile is skewed to the lateral side, but postendarterectomy it skews in the medial direction. After endarterectomy the velocity profile becomes more symmetric. Velocity values close to the lateral wall are higher than those near the medial wall for both pre- and postendarterectomy artery. Maximum velocity values are observed in the center lumen.

Diastole. Velocities at early diastole are higher laterally than medially, by 13 cm/s and 4 cm/s pre- and postendarterectomy, respectively. Before endarterectomy, the maximum velocity at early diastole is observed at the mid-distance between the lateral wall and the center lumen. Postendarterectomy, at late diastole the velocity increases. After endarterectomy, both end diastolic and late diastolic velocity profiles become more smooth and symmetric, with maximum velocities observed in the center lumen.

Variability between the patients

Variability of the velocity profiles between the patients was studied by calculating the standard deviations of the mean velocity profiles plotted on Figs 2-4. For brevity, we present the results only for the postendarterectomy peak

systolic and late diastolic measurements. As demonstrated in Fig 5, there is appreciable variability in the velocity profiles between the patients for all three carotid artery branches. However, the main characteristics of the velocity profiles described above are valid for the majority of the subjects.

Three-dimensional blood velocity profiles

Three-dimensional blood velocity profiles were constructed from the data presented in Figs 2-4 by interpolating the velocities between each point of measurement (Fig 1). Fig 6 presents the mean three-dimensional peak systolic velocity profiles in the postendarterectomy CCA, ICA, and ECA. As before, the arterial lumen was normalized to a circle 1 cm in diameter. Velocity profiles in all three carotid artery branches were not symmetric about the arterial centerline.

DISCUSSION

Despite the well-known association of atherosclerosis with systemic risk factors, lesions tend to occur focally in regions of the arterial tree demonstrating disturbed flow. Numerous studies^{1,16} suggest that certain hemodynamic factors, particularly low and oscillating wall shear stress,

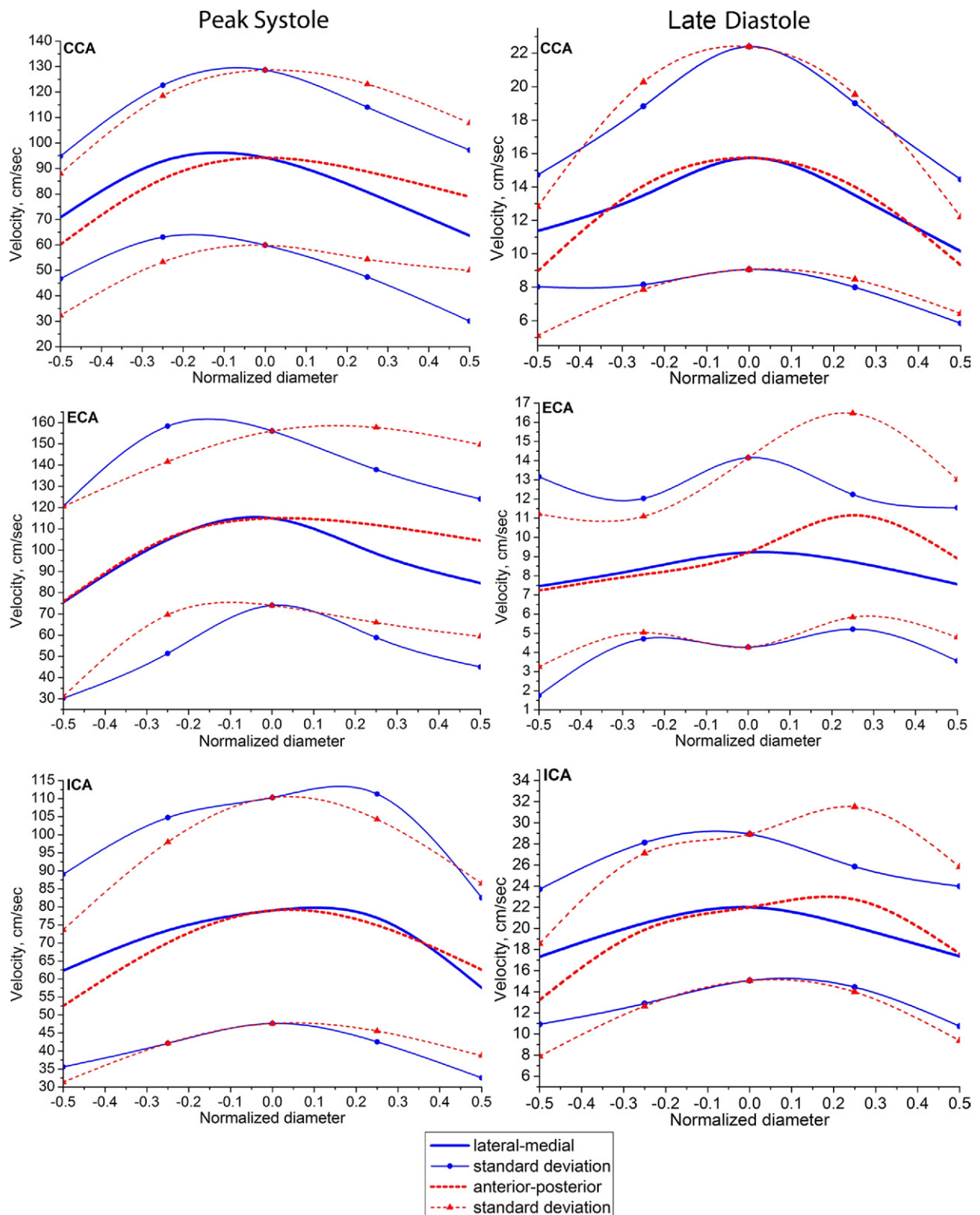


Fig 5. Mean velocity profiles in the lateral-medial and anterior-posterior directions for common (CCA), external (ECA), and internal (ICA) postendarterectomy carotid artery at peak systole and late diastole. Standard deviations are plotted along with mean values to show the variability of data. Horizontal axis represents the diameter of the artery normalized to 1 cm.

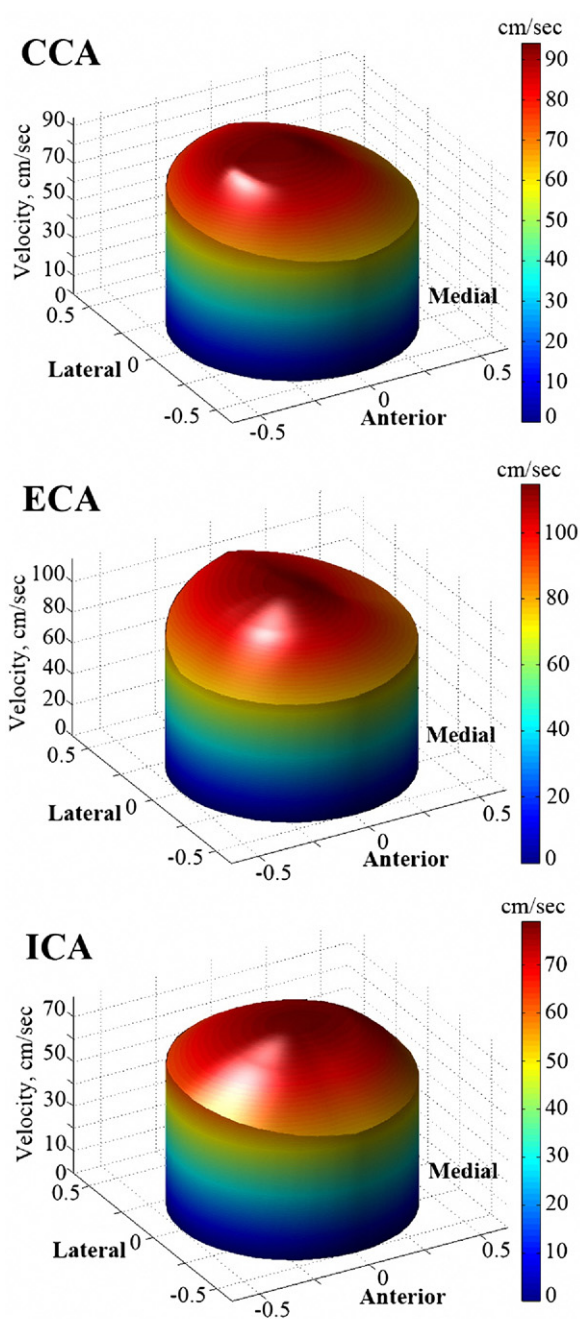


Fig 6. Postendarterectomy three-dimensional velocity profiles in the common (CCA), external (ECA), and internal (ICA) carotid arteries at peak systole.

contribute to the initial localization of atherosclerotic plaque and to the development of restenosis and treatment failure following operative or percutaneous intervention. In the disease prone carotid bulb, direct measurement of blood flow characteristics is difficult, and numerical modeling is frequently used to simulate and study the bulb's unique hemodynamic conditions. When combined with

geometry data, numerical modeling can predict the hemodynamics within the bulb utilizing laminar blood flow measurements taken proximal and distal to areas of flow disturbance. However, in order for numerical models to make accurate predictions, input and output boundary conditions must also be accurate.

Using duplex ultrasonography, we obtained multiple measurements of blood velocity profiles from the inflow and outflow segments of in vivo human carotid artery bifurcations. Our findings of skewed velocity profiles at all three locations during both systole and diastole contradict the common assumption that blood velocity profiles away from the bulb are symmetric about the arterial axis.^{3,4,11} However, our results are in agreement with findings obtained using magnetic resonance imaging of the CCA⁶⁻⁸ also describing skewed profiles. We speculate that the observed skewing of the velocity profile in vivo may be due to tortuosity of the artery and cross-sectional asymmetry of the flow lumen.²⁻⁴ It has been previously reported^{6,8} that even though distal CCA appears to be relatively straight, its curvature is still sufficient for significantly skewing the velocity profile. In particular, it has been suggested that the bend provokes a radial redistribution of momentum to compensate the centrifugal force that, in turn, even in steady flow conditions, yields consistent velocity profile skewing.^{6,17,18} A detailed investigation of the influence of arterial tortuosity on the velocity profile shape is beyond the scope of the present study. However, the geometries of the arteries in this patient group are being currently analyzed by our team. Preliminary results reveal strong nonplanarity and both in- and out-of-plane curvature of the considered arteries.

It has also been suggested that skewing of the velocity profile may correspond to the presence of secondary flows.⁶ From duplex measurements alone it is not possible to infer the value of the secondary velocity components. However, it has been reported¹⁹ that secondary velocities are <10% of the axial velocity in physiologically curved tubes. Such low value therefore indicates that skewing of the velocity profile may be due to presence of the secondary flows, rather than their strength.⁶

Velocity profiles in all arteries were skewed posteriorly both before and after endarterectomy. In the mediolateral direction, the CCA velocity profile is skewed with higher velocities laterally. Similar results for the CCA profile were recently reported.^{7,8} In the ECA, the velocity profile is also skewed laterally, with velocities near the medial wall being higher than those near the lateral wall. The opposite was observed in the ICA, where the velocity profile was skewed medially, but with higher velocities measured near the lateral wall than the medial wall. The finding that velocity profiles tend to be skewed to the inner walls of the bifurcation has been reported previously.^{2,8,14,18} However, in these studies, velocity profiles were evaluated close to the bulb and therefore were affected by branching. Our findings demonstrate that profiles do not regain symmetry even after 4 to 5 diameters off the flow divider, where they are usually assumed symmetric. Overall, the shapes of the ve-

locity profiles postendarterectomy were found to become more smooth and symmetric.

As expected, pre- and postendarterectomy velocity values were considerably different. After endarterectomy, velocities increased in both the CCA and ICA, but decreased in the ECA. This finding is likely due to the flow changes produced by the endarterectomy. Before endarterectomy, the flows through the CCA and ICA are diminished because of the stenosis in the ICA, with much of the outflow accommodated by the high resistance ECA vascular bed. The endarterectomy removes the atherosclerotic plaque blocking the ICA that serves the low resistance vascular bed in the brain, and as a result the total flow through the ICA and CCA increases, while the previously higher flow in ECA decreases. Increase in the CCA and ICA flow produced by endarterectomy has been reported to play an important clinical role by improving perfusion to the areas of the brain with marginal circulation and contributing to maintenance of healthy cerebral function.²⁰⁻²³ Interestingly, throughout the majority of the cardiac cycle, velocities in the CCA and ICA were higher after endarterectomy with the exception of early diastole. It is probable that the latter exception may be due to return of the waveform to a more “normal” shape, which, among other things, features a downfall in the velocity values at early diastole.

Our data did not show the presence of flow inversion during diastole neither in CCA nor in ICA or ECA but have demonstrated M-shaped velocity profiles with decreased velocity in the center lumen for some patients. In a straight rigid tube, flow inversion can occur during flow deceleration because of the excessive static pressure recovery close to the walls where kinetic energy is low. Velocity components of the flow in the straight tube are mainly axial, while curved shape of the genuine carotid artery promotes development of secondary velocity components which increase the kinetic energy of the flow close to the walls. This kinetic energy can be converted into static pressure in the deceleration phase, thereby decreasing the risk of flow inversion.⁶ However, this may not be enough to prevent the velocity profile from taking the M-shape during deceleration, which has been observed in some patients.

Our findings seem to contradict the commonly accepted “no-slip” boundary condition at the walls of the artery.²⁴ This condition is dictated by the viscous nature of blood and states that blood velocity at the boundary with arterial wall has zero value. Instead of showing gradual decrease of velocity approaching the arterial wall, some of our measurements show a perplexing increase in velocity values. Although additional research is needed to fully investigate this phenomenon, this observation may be associated with (a) measurement of velocities near but not exactly against the arterial wall and (b) wall motion due to pulsation that could interact with the measurements. Use of higher resolution duplex devices or methods of measurement that are less operator-dependent (such as magnetic resonance imaging) may provide further insight into the nature of velocity changes against the walls of arteries.

The global burden of stroke presents a pressing need for improved understanding of the mechanisms involved in the pathophysiology and treatment of carotid bifurcation disease. Our work demonstrates the importance of considering the entire three-dimensional pulsatile velocity profiles and provides a detailed quantification of the velocity profiles present at the inflow and outflow boundaries of the pre- and postendarterectomy human carotid bifurcation. The in vivo hemodynamics of these human carotid artery segments are considerably different from those previously generated by in vitro and computer-based models. These detailed in vivo data can be used to design better numerical models that more closely replicate in vivo hemodynamic conditions. These models can help us delineate the association between the complex flow patterns present in the carotid bulb and carotid bifurcation disease, such as atherosclerosis and restenosis, and may also permit in silico development, testing, and optimization of vascular devices to treat disease in the carotid bifurcation.

AUTHOR CONTRIBUTIONS

Conception and design: AK, YD, JM, IP
Analysis and interpretation: AK, YD, JM, IP
Data collection: AK, IP, AD
Writing the article: AK, YD, JM, IP
Critical revision of the article: AK, YD, JM, AD, IP
Final approval of the article: AK, YD, JM, AD, IP
Statistical analysis: AK
Obtained funding: Not applicable
Overall responsibility: IP

REFERENCES

1. Malek AM, Alper SL, Izumo S. Hemodynamic shear stress and its role in atherosclerosis. *JAMA* 1999;282:2035-42.
2. Berger SA, Jou LD. Flows in stenotic vessels. *Annu Rev Fluid Mech* 2000;32:347-84.
3. Perktold K, Rappitsch G. Computer simulation of local blood flow and vessel mechanics in a compliant carotid artery bifurcation model. *J Biomech* 1995;28:845-56.
4. Van Steenhoven AA. Physics of heart and circulation: velocity profiles in large arteries. Bristol, United Kingdom: Institute of Physics Publishing; 1993. p. 295-320.
5. Kamenskiy AV, Pipinos DAS II, Salkovskiy YE, Yu Kossovich L, Kirilova IV, Bockeria LA, et al. Finite element model of the patched human carotid. *Vasc Endovasc Surg* 2009;43:533-41.
6. Tortoli P, Michelassi V, Bambi G, Guidi F, Righi D. Interaction between secondary velocities, flow pulsation and vessel morphology in the common carotid artery. *Ultrasound Med Biol* 2003;29:407-15.
7. Sui B, Gao P, Lin Y, Qin H, Liu L, Liu G, et al. Noninvasive determination of spatial distribution and temporal gradient of wall shear stress at common carotid artery. *J Biomech* 2008;41:3024-30.
8. Ford MD, Xie YJ, Wasserman BA, Steinman DA. Is flow in the common carotid artery fully developed? *Physiol Meas* 2008;29:1335-49.
9. Schulz UG, Rothwell PM. Major variation in carotid bifurcation anatomy: a possible risk factor for plaque development? *Stroke* 2001;32:2522-9.
10. Lee SW, Antiga L, Spence JD, Steinman DA. Geometry of the carotid bifurcation predicts its exposure to disturbed flow. *Stroke* 2008;39:2341-7.
11. Chen J, Lu XY. Numerical investigation of the non-Newtonian pulsatile blood flow in a bifurcation model with a non-planar branch. *J Biomech* 2006;39:818-32.

12. Kane AG, Dillon WP, Barkovich AJ, Norman D, Dowd CF, Kane TT, et al. Reduced caliber of the internal carotid artery: a normal finding with ipsilateral absence or hypoplasia of the A1 segment. *AJNR Am J Neuroradiol* 1996;17:1295-301.
13. Krejza J, Arkuszewski M, Kasner SE, Weigle J, Ustymowicz A, Hurst RW, et al. Carotid artery diameter in men and women and the relation to body and neck size. *Stroke* 2006;37:1103-5.
14. Bassini M, Gatti E, Longo T, Martinis G, Pignoli P, Pizzolati PL, et al. In vivo recording of blood velocity profiles and studies in vitro of profile alterations induced by known stenoses. *Tex Heart Inst J* 1982;9:185-94.
15. Keller HM, Meier WE, Anliker M, Kumpe DA. Noninvasive measurement of velocity profiles and blood flow in the common carotid artery by pulsed Doppler ultrasound. *Stroke* 1976;7:370-7.
16. Ku DN, Giddens DP, Zarins CK, Glagov S. Pulsatile flow and atherosclerosis in the human carotid bifurcation. Positive correlation between plaque location and low oscillating shear stress. *Arteriosclerosis* 1985;5:293-302.
17. Rindt C, VanSteenhoven A, Janssen J, Vossers G. Unsteady entrance flow in a 90 deg curved tube. *J Fluid Mech* 1991;226:445-74.
18. Van Langenhove G, Wentzel JJ, Krams R, Slager CJ, Hamburger JN, Serruys PW, et al. Helical velocity patterns in a human coronary artery: a three-dimensional computational fluid dynamic reconstruction showing the relation with local wall thickness. *Circulation* 2000;102:E22-4.
19. Krams R, Bambi G, Guidi F, Helderma F, van der Steen AFW, Tortoli P, et al. Effect of vessel curvature on Doppler derived velocity profiles and fluid flow. *Ultrasound Med Biol* 2005;31:663-71.
20. Wiberg J, Normes H. Effects of carotid endarterectomy on blood flow in the internal carotid artery. *Acta Neurochir* 1983;68:217-26.
21. Boysen G, Ladegaard-Pedersen HJ, Valentin N, Engell HC. Cerebral blood flow and internal carotid artery flow during carotid surgery. *Stroke* 1970;1:253-60.
22. Perry PM, Drinkwater JE, Taylor GW. Cerebral function before and after carotid endarterectomy. *Br Med J* 1975;4:215-6.
23. Fearn SJ, Hutchinson S, Riding G, Hill-Wilson G, Wesnes K, McCollum CN, et al. Carotid endarterectomy improves cognitive function in patients with exhausted cerebrovascular reserve. *Eur J Vasc Endovasc Surg* 2003;26:529-36.
24. McDonald D. Blood flow in arteries. London: Edward Arnold (Publishers) Ltd; 1974.

Submitted Nov 10, 2010; accepted Mar 21, 2011.